Journal of Applied Microbiology ISSN 1364-5072

REVIEW ARTICLE

The prion/lipid hypothesis – further evidence to support the molecular basis for transmissible spongiform encephalopathy risk assessment

P. Gale

Tilehurst, Reading, Berkshire, UK

Keywords
dose–response, formaldehyde, inactivation, incubation period, protein/lipid interactions, risk assessment, sphingolipid,transmissible spongiform encephalopathy.

Correspondence
P. Gale, 59, Fairway Avenue, Tilehurst, Reading, Berkshire, RG30 4QB, UK.
E-mail: pg@microbiologicalriskassessment.com

2007/0051: received 12 January 2007, revised 17 March 2007 and accepted 25 March 2007

doi:10.1111/j.1365-2672.2007.03411.x

Summary

Defining the molecular structure of the transmissible spongiform encephalopathy (TSE) agent is important both for underpinning risk assessments and for developing and understanding decontamination strategies. Recent studies have shown that oligomeric particles comprising 14–28 prion protein (PrP) molecules are much more infectious than larger fibrils (prion rods) or indeed smaller oligomers (trimers) and PrP monomers. Here, results from deactivation studies (with alkali, heat, hexane or formaldehyde) are interpreted in terms of the infectious nucleation seed comprising 14–28 PrP molecules held together by interactions with amphipathic phospholipid (PL) or more probably sphingolipid (SL) from the host. According to the PrP/lipid hypothesis, the strength of the protein/lipid interactions accounts for the high thermostability of TSE infectivity and for differences in thermostability between strains. The implications of the molecular biophysics data for environmental TSE risk assessments are discussed with respect to behaviour in soil. While formaldehyde appears to cause inactivation of scrapie infectivity by increasing the ID_{50}, the dose–response is complicated by apparent heterogeneity between hamster subpopulations in susceptibility. The process of inactivation by formaldehyde may be due to cross-linking the highly infectious 14–28 PrP oligomers into larger, but less infectious aggregates. This process appears more reversible in some hamster subpopulations than others.

Introduction

The transmissible spongiform encephalopathies (TSEs) are a group of progressive neurological prion diseases of mammals, including scrapie in sheep and goats, Creutzfeldt–Jakob disease (CJD) in humans, bovine spongiform encephalopathy (BSE) in cattle, and chronic wasting disease (CWD) in deer and elk. In these diseases (Prusiner 2004), the cellular isoform of the prion protein (PrP^{C}) is post-translationally misfolded into the infectious disease-related form denoted as PrP^{Sc} (for scrapie prions) or PrP^{RES} (to represent its greater resistance to protease digestion). PrP^{C} is encoded by the *PrP* gene and is a cell surface glycosyl-phosphatidylinositol-anchored protein, which is particularly abundant in neurons (Taylor and Hooper 2006). Although there are glycosylation differences between the PrP^{C} and PrP^{Sc} isoforms (Rudd *et al.* 1999), nuclear magnetic resonance (NMR) studies of bovine PrP^{C} suggest that underglycosylation of PrP^{C} does not facilitate the conversion of PrP^{C} to PrP^{Sc} (Hornemann *et al.* 2004). The oligosaccharides near the *N*-glycosidic linkages are flexible and dynamic, and one function of the sugars could be to protect extensive regions of the protein surface from intermolecular contacts (Hornemann *et al.* 2004).

Scrapie has been recognized in Europe since the 18th century (Prusiner *et al.* 2004). BSE was first recognized in November 1986 in the UK (Wells and Wilesmith 2004). Up to December 2006, over 179 145 cases of BSE have been confirmed in cattle in UK (http://www.defra.gov.uk/

animalh/bse/statistics/incidence.html). The epidemic was accelerated by recycling of infected bovine tissues through the use of meat and bone meal in feed prior to the ruminant feed ban in July 1988 (Kimberlin and Wilesmith 1994; Anderson *et al.* 1996; Wells and Wilesmith 2004). The incidence of BSE in cattle in the UK peaked in 1992 with 36 680 confirmed cases (Comer and Huntly 2004). BSE infectivity is localized to the brain, spinal cord and other offals in infected cattle (Kimberlin 1996; Comer and Huntly 2004). It is estimated that 446 000 infected cows entered the human food chain before the use of specified bovine offal in food for human consumption was banned in November 1989, with another 283 000 more before the end of 1995 (Anderson *et al.* 1996). In March 1996, it was announced that a new and distinct variant of CJD (vCJD) in humans could be linked to BSE in cattle (Anderson *et al.* 1996). The number of deaths from definite or probable vCJD in the UK is 158 (to 1 December 2006) with another six still alive (http://www.cjd.ed.ac.uk/figures.htm).

It is not yet clear how many people will eventually develop vCJD as a result of eating beef products from cattle infected with BSE. In the UK, all 161 cases of vCJD (to April 2006) have been in people homozygous for the *PrP* gene with methionine at codon 129 (Ironside *et al.* 2006). The methionine homozygous genotype makes up 40% of the population (Ironside *et al.* 2006). In a prevalence study for vCJD, Ironside *et al.* (2006) identified three appendixes that stained positive for disease-associated PrP in a total of 12 674 specimens (11 109 appendixes and 1565 tonsils). Extracted DNA from two of those three appendixes confirmed the PrP genotype as homozygous for valine at codon 129. DNA analysis could not be performed on the third appendix. This genotype makes up 10% of the population. So far, no clinical cases of vCJD have been found in valine homozygous individuals. However, the results of Ironside *et al.* (2006) give the first indication that valine homozygotes may be susceptible to vCJD. Those authors concluded that people homozygous for valine at condon 129 of the *PrP* gene and infected with vCJD may have a prolonged incubation period (IP), during which horizontal spread of the infection could occur from blood donations or from contaminated surgical instruments. Formaldehyde does not decomtaninate prion-infected materials (McDonnell and Burke 2003). The vulnerability to BSE of the remaining 50% of the population, who are heterozygous at codon 129, is not yet known. Recently, a case of vCJD was detected in a heterozygous individual infected through a blood transfusion resulting in exposure to vCJD prions (Peden *et al.* 2004). The risk of vCJD through blood transfusion is currently of concern with recent reports of three cases arising from a single individual donor (Dietz *et al.* 2007).

Risk assessments for prion diseases have always been hampered by the lack of a clear definition of the nature and structure of the infectious agent, and in particular whether its mode of action is independent or co-operative (i.e. with a threshold dose). Indeed, quantitative BSE risk assessments have relied simply on estimates of the mass of material comprising an ID_{50} (Kimberlin 1996; Gale *et al.* 1998; Comer and Huntly 2004). Understanding the exact nature of the molecular structure and composition of the infectious agent in prion diseases will help develop procedures to achieve more effective destruction of infectivity (e.g. on surgical instruments). Previously, it was proposed that the unit of infectivity for prion disease is a nucleation seed comprised of PrP and host phospholipid (PL), with the strength of the protein/lipid interactions controlling the thermostability (Gale 2006a). As yet there are no data which positively identify a second component, and if a host lipid is involved, it is more likely to be host sphingolipid (SL) rather than PL. Thus, PrP^{C} has an SL-binding domain (Taylor and Hooper 2006). Indeed, PrP^{C} shares an SL-binding domain with HIV-1 surface envelope glycoprotein gp120 and Alzheimer's β-amyloid peptide (Mahfoud *et al.* 2002).

The principles of protein/lipid interactions are the same whether the lipid is PL or SL as both are amphipathic molecules. Sphingolipids enable highly specific interactions and binding between proteins. As an example, the glycosphingolipid, α-galactosylceramide, is the most potent natural killer T cell (NKT) activator (Wu *et al.* 2006), mediating specific interaction between the antigen presenting CD1d molecule and the T-cell receptors on the NKT cell. Thus, it could be envisaged that PrP^{Sc}/SL interactions within the TSE agent nucleation seed could be highly specific (depending on the 3D structure of PrP^{Sc}) accounting for the both high thermostability of the TSE agent and differences between strains in thermostability as proposed previously (Gale 2006a). In that study, IP data were interpreted in terms of the nucleation seeds in untreated material initiating infection through independent action, with treatments such as alkali and autoclaving disrupting the protein/lipid interactions and degrading the lipid, thus breaking up the nucleation seeds into smaller PrP units, or even PrP monomers, which require co-operative interactions at low doses giving much longer IPs. In this paper, further evidence is reviewed in relation to the importance of lipid. This includes interpretation of published observations from various inactivation studies using NaOH, heat, organic solvent and formaldehyde. The prion/lipid hypothesis fits with the growing body of evidence that the lipid bilayer membrane plays a central role in the mechanism of conversion of PrP^{C} to PrP^{Sc} (Kazlauskaite and Pinheiro 2005; Taylor and Hooper 2006).

Molecular models for prion rods and hexagonal 2D-arrays

In the molecular models of Govaerts *et al.* (2004) and Langedijk *et al.* (2006), the basic structural unit is a trimer of PrP^{Sc}, i.e. three identical PrP^{Sc} molecules, held together into a flat cylindrical disc. The trimer is the basic building block. The trimers can either stack like a vertical column of coins into a long 1D rod (fibril) or, like coins spread out on a flat table, can order into 2D arrays with hexagonal packing (2D-hexagonal arrays). In each PrP^{Sc} monomer, the polypeptide backbone is proposed to be folded into a left-handed β-helix, which is essentially a β-sheet secondary structure wrapped around itself through helical turns (Govaerts *et al.* 2004).

Two-dimensional (2D) hexagonal arrays

Resemblance of 2D-arrays of PrP^{Sc} to bacteriorhodopsin in Halobacterium halobium purple membrane

The integral membrane protein bacteriorhodopsin (BR) in purple membrane from *H. halobium* has certain similarities to PrP^{Sc}. Firstly, BR is of similar size to PrP with molecular weights of 26 kDa (Henderson and Unwin 1975) and 27–33 kDa (Gabizon *et al.* 1988), respectively. Secondly, BR forms trimers within lipid bilayer membranes (Grigorieff *et al.* 1995). Thirdly, the BR trimers pack into the characteristic paracrystalline, hexagonal 2D-arrays of purple membrane (Blaurock and Stoeckenius 1971). Sabra *et al.* (1998) have proposed a model for lipid-mediated 2D array formation of membrane proteins based on BR. It is well established for BR that both high protein content and the presence of specific purple membrane PLs are required for formation of well-ordered 2D aggregates (Sternberg *et al.* 1989, 1992). BR is comprised of seven transmembrane α-helices (Henderson and Unwin 1975; Henderson *et al.* 1990) instead of the left-handed β-helix proposed for PrP^{Sc} (Govaerts *et al.* 2004; Langedijk *et al.* 2006). Seven PL molecules (in bilayer configuration) are associated with each BR molecule in the purple membrane (Kates *et al.* 1982). Grigorieff *et al.* (1995) identified six lipid sites per BR molecule in the crystal form.

PrP^{Sc} may be associated with five lipid molecules in 2D-arrays

The question to be answered is how many lipid molecules are there around each PrP^{Sc} molecule in the 2D-arrays. The answer may come from studies with sodium dodecyl sulphate (SDS). SDS at low concentrations (below the critical micelle concentration) does not act as a denaturing detergent for PrP, but as a specific ligand (Leffers *et al.* 2004) competing for hydrophobic sites between PrP molecules. Leffers *et al.* (2004) showed that at least four different classes of binding sites for SDS exist on PrP. According to Leffers *et al.* (2004), at least five SDS molecules have to interact with PrP to switch the confirmation from a PrP^{C}-like state to a PrP^{Sc}-like state. In particular, β-structured multimers of PrP^{Sc} show very strong binding of five SDS molecules per PrP molecule (Leffers *et al.* 2004). These are depicted as hexagonal arrays of PrP^{Sc} with SDS molecules at the interfaces in Fig. 7 of Leffers *et al.* (2004). It is possible that the structured multimers studied by Leffers *et al.* (2004) are 2D arrays of hexagonally packed PrP^{Sc} in which the lipid molecules have been replaced by SDS molecules. This would suggest that each PrP^{Sc} molecule in the 2D array is associated with five lipid molecules, which is similar to the six or seven associated with each BR molecule in purple membrane (Kates *et al.* 1982; Grigorieff *et al.* 1995). Interestingly, with just five SDS molecules per PrP, Leffers *et al.* (2004) reported irreversible aggregation of the PrP into insoluble multimers. This could be analogous to BR forming extensive sheets of 2D-hexagonally packed trimers (Blaurock and Stoeckenius 1971; Grigorieff *et al.* 1995), although the PrP^{Sc} 2D-arrays do not appear so extensive or well-ordered (Fig. 1 E of Wille *et al.* 2002) and may break up into smaller units, e.g. 14–28 PrP oligomers. This raises the question of what happens at the edges of those oligomers, i.e. at the hydrophobic interface with water. Leffers *et al.* (2004) depict SDS molecules at the edges of the oligomer, as in a micelle. It is possible that the *N*-linked oligosaccharide plays a role in protecting the exposed hydrophobic regions at the edges of the oligomers in the 2D-arrays. BR being a bacterial protein does not have

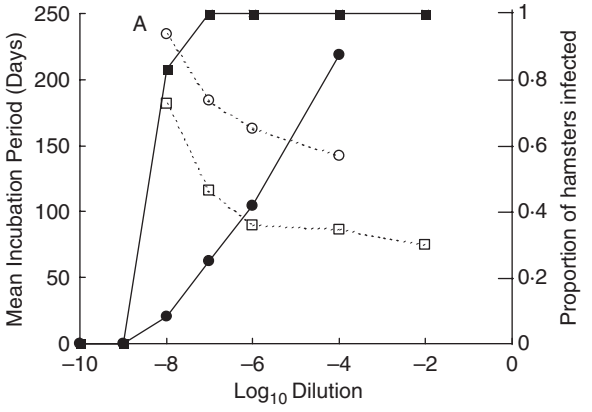

Figure 1 Titration of homogenized brain pool of 263 K strain of hamster-adapted scrapie agent in hamsters. Solid lines with filled symbols show proportions of hamsters infected as a function of dilution of brain homogenate with (circles) and without (squares) formaldehyde fixation. Incubation periods (dashed line with hollow symbols) are also shown. Plotted from data taken from Brown *et al.* (2000). Point A represents IP data for just one hamster, the other IP points are averages.

covalently attached oligosaccharides, and forms much more extensive arrays.

More SDS molecules are associated with PrP monomers
Partial denaturation of PrP starts only after binding of about 30 SDS molecules per PrP molecule (Leffers *et al.* 2004). This would represent the fully monomeric PrP. Using electron spin resonance (ESR) spectroscopy (Gale 1993) estimated the number of PL molecules in the boundary layer (i.e. the shell of lipids in immediate contact with the protein surface and immobilized on the ESR time scale) for fully dispersed monomeric BR to be 18–21. This is similar to the 21 SDS molecules associated with dimeric PrP (Leffers *et al.* 2004). Although monomeric PrP is associated with 31 SDS molecules, the PrP is partially denatured (which would take up additional SDS molecules) so dimeric PrP is a better comparison in this respect. When packed into the 2D hexagonal arrays in purple membrane, there are only six or seven lipid molecules per 26 kDa BR monomer (Kates *et al.* 1982; Grigorieff *et al.* 1995). This reflects the displacement of the PLs from the boundary shell of BR on formation of protein/protein contacts during trimer formation and the subsequent packing of the trimers into the 2D hexagonal lattice. A soluble oligomeric PrP intermediate, with the β-structure, is composed of 12–14 PrP molecules and requires binding of about 19 or 20 SDS molecules per PrP molecule (Leffers *et al.* 2004). The extra SDS molecules are required around the edges of the oligomer. This structure could resemble the highly infectious 14–28 PrP oligomers reported by Silveira *et al.* (2005).

Prion rods and fibrils

A 3D structure of the prion rod has been proposed based on stacking of prion trimer disks (Govaerts *et al.* 2004; Langedijk *et al.* 2006). Inspection of the proposed structure would suggest that lipids are not required for stabilization. This is consistent with prion rods containing only 1% (mol/mol) SL, i.e. just one molecule of host SL for every 99 PrP^{Sc} molecules (cited in Appel *et al.* (2001)). Thus, the prion rods have some 700-fold fewer lipid molecules (per PrP) than would be expected for an integral membrane protein (i.e. BR) of similar size. This suggests that the trimers in the rods are held together predominantly by protein/protein interactions and is consistent with the new two-rung model of Langedijk *et al.* (2006) in which the β-helices stack between adjacent trimers in the fibril.

A molecular mechanism for conversion of rods into 14–28 PrP particles: the role of *N*-linked oligosaccharide

Prions rods can be reversibly dispersed into PL liposomes using detergent and chloroform/methanol extraction (Gabizon *et al.* 1988). The *N*-linked oligosaccharides could play a role in stabilizing the PrP^{Sc} trimers in the rod form and feature prominently in the 3D structure proposed for the prion rod (Govaerts *et al.* 2004). Oligosaccharides have both hydrophobic and hydrophilic faces. Thus, in the rods, the hydrophobic faces of the oligosaccharides could protect the hydrophobic transmembrane portions of the trimers which otherwise would be exposed to the aqueous medium. In effect, the *N*-linked oligosaccharides would replace the amphipathic lipid or protein contacts proposed in the hexagonal 2D array structure. The *N*-linked sugars extend away from the centre of the rod structure providing a hydrophilic surface for interaction with the water molecules and forming a sugar backbone or scaffold (Appel *et al.* 2001). The *N*-linked oligosaccharides are highly flexible (Hornemann *et al.* 2004) and often function to protect proteins. In the 14–28 PrP oligomers, the oligosaccharides would be displaced away from the plane of the 2D arrays, allowing hexagonal packing of trimers through protein/lipid interactions between adjacent trimers. As the 14–28 PrP oligomers are more infectious than the rods (Silveira *et al.* 2005), any stabilization of the rods by oligosaccharide would not be expected to stabilize the agent or strain.

Evidence supporting the nucleation seed

Caughey and Lansbury (2003) review experimental studies aimed at identification and characterization of the neurotoxic protein aggregates in neurodegenerative diseases including Alzheimer and Parkinson's and the TSEs. They report the emerging notion that an ordered prefibrillar oligomer, or protofibril, may be responsible for cell death, and that the fibrillar form that is typically observed at autopsy may actually be neuroprotective. They add that most PrP oligomers *in vivo* are likely to be attached to cellular membranes and so are not readily visible ultrastucturally as fibrils, and when constrained by attachment to membrane surfaces, PrP^{RES} oligomers may preferentially form ordered 2D arrays perhaps like those observed by Wille *et al.* (2002). Membrane-bound PrP^{RES} may only become overtly fibrillar or plaquelike after extraction from membranes by some in known process *in vivo*, or by detergent extraction *in vitro*.

The work of Silveira *et al.* (2005) identifying the most infectious particles

Silveira *et al.* (2005) fractionated aggregates of PrP^{RES} according to size, with larger fraction numbers representing larger aggregates comprising more PrP molecules. The properties of the main fractions are summarized

Table 1 Summary of properties of PrP aggregate fractions studied by Silveira *et al.* (2005)

Fraction	Structural unit (fraction)	Number of PrP molecules	Specific infectivity	Incubation period (day)
6	Monomers and trimers	1 or 3	Virtually absent	119
7			3000-fold lower than fraction 12	119
12	Larger oligomers	14–28	Highest	91
21	Intermediate fibrils	~300	70-fold lower than fraction 12	91
26	Larger fibrils and rods	~1000	Low	91

in Table 1. Silveira *et al.* (2005) calculated a 'specific infectivity' relative to the PrP content of the aggregates comprising each fraction.

Particles comprising 14–28 PrP molecules are the most infectious PrP particles while monomers and larger fibrils have low specific infectivity

The highest specific infectivity was recorded for fraction 12 dropping off steeply for the fractions to each side. Indeed, the specific activity for fraction 7 (small oligomers) was ~3000-fold lower than that for fraction 12, and the large aggregates in fraction 23 had 70-fold lower-specific infectivity (Table 1). Silveira *et al.* (2005) visualized the sizes and shapes of the PrP aggregates in various fractions. Fraction 26 contained long fibrils, and fraction 21 shorter fibrils. Fractions 10 and 15 (on either side of fraction 12) contained spherical particles and no fibrils. Those authors concluded that the most infectious particles are ~17–27-nm diameter and 300–600-kDa molecular weight, corresponding to an oligomer of 14–28 PrP molecules.

Co-operative action on disruption of the nucleation seed: particles of fewer than five PrP molecules not only have lower specific infectivities, but also longer IPs

On the basis of interpretation of IP data, Gale (2006a) proposed that breaking up the nucleation seed into smaller subfragments (containing intact PrP molecules) shifted the mode of infection from independent action to co-operative action. Thus, much longer IPs are observed at low doses below the ID_{50} and could reflect co-operative action for any PrP^{Sc} surviving in autoclaved or alkali-treated material (Taylor and Fernie 1996; Taylor *et al.* 2002). The work of Silveira *et al.* (2005) is particularly helpful here because it demonstrated that the IP is increased for monomers or small oligomers (<5 PrP molecules) compared with larger oligomers (14–28 PrP molecules) and the larger fibrils. The IPs for the various fractions are summarized in Table 1. This is consistent with the interpretation that disruption of the nucleation seed by rendering or alkali treatment gives small oligomers or even monomers, which initiate infection through a co-operative mechanism (Gale 2006a).

Autoclave inactivation studies with formaldehyde support the concept of the nucleation seed

McDonnell and Burke (2003) note that biocides that can potentially cross-link proteins (including glutaraldehyde and formaldehyde) should not be used to decontaminate prion-infected materials or devices. Indeed, formaldehyde fixation increases resistance to autoclave inactivation (Taylor and McConnell 1988; Brown *et al.* 1990). This observation can be interpreted in terms of the concept of a nucleation seed initiating infection through independent action. Thus, cross-linking by formaldehyde prior to autoclaving holds the PrP molecules comprising the 14–28 PrP oligomer nucleation seed together preventing disruption of the protein/lipid interactions by autoclaving and hence inactivation of the nucleation seed by molecular dispersion. This is consistent with formaldehyde cross-linking only enhancing thermostability if applied before autoclaving as opposed to after (Brown *et al.* 1990). Indeed, treatment with formaldehyde after autoclaving may even increase the deactivation. Thus, formaldehyde fixation followed by autoclaving gives just a 1·8-log reduction in infectivity titres of scrapie-infected hamster brain. Autoclaving alone gave a 5·3-log reduction, while autoclaving followed by formaldehyde fixation gave a 6·3-log reduction (Brown *et al.* 1990). It is proposed that the extra reduction through formaldehyde fixation after autoclaving is due to linking the most infectious 14–28 PrP particles into larger aggregates of lower infectivity according to the data from Silveira *et al.* (2005). Indeed, formaldehyde alone gave a 1·5-log reduction (Brown *et al.* 1990).

Formaldehyde does not appear to increase resistance to dry heat at 600°C

Brown *et al.* (2000) note that compared with wet heat treatment (autoclaving), formaldehyde treatment does not protect against dry heat (ashing) in experiments with the hamster adapted 263 K strain of scrapie. Exposure of brain homogenate to 600°C produced a flaming tissue combustion that lasted several seconds, and yielded a residue of glowing black ash that had lost 98–99% of its initial weight. The undiluted brain homogenate (dry heated without prior

formaldehyde fixation) infected five of 18 hamsters. In contrast, only one of 24 hamsters was infected with brain homogenate which was fixed with formaldehyde prior to heating. If formaldehyde protected against dry heat, more hamsters would have been infected. The difference between wet and dry heat can perhaps be explained by considering the nature of the hydrophobic interactions which hold the PrP molecules together within a nucleation seed. Hydrophobic interactions are particularly important for maintaining protein/lipid interactions, and are also important in protein/protein interactions. The hydrophobic effect is driven by the entropy of the surrounding water molecules. The dry heat at 600°C will drive off all the water so weakening the hydrophobic interactions which hold the nucleation seed together, such that the formaldehyde cross-linking is no longer sufficient alone to hold the seed together. In contrast, the hydrophobic interactions will still be maintained with wet heat (autoclaving), and the seed further stabilized by formaldehyde cross-linking.

The effect of formaldehyde on the dose–response

Data on the effect of formaldehyde on unheated scrapie-infected hamster brain homogenate are taken from Tables 2 and 3 of Brown *et al.* (2000) and plotted in Fig. 1. Overnight fixation with formaldehyde increases the ID_{50} by the order of three-logs, shifting the dose–response curve to the right. However, formaldehyde fixation also changes the shape of the dose–response curve, giving a shallower slope around the ID_{50}. The findings of Silveira *et al.* (2005) raise the question of whether formaldehyde increases the ID_{50} (Fig. 1) simply by cross-linking the highly infectious 14–28 PrP oligomers into larger aggregates with lower specific infectivities (Table 1). Formaldehyde could also stabilize the fibrils by cross-linking the reactive functional groups on adjacent trimer units in the rod. The oligosaccharide forms a rigid scaffold or backbone (Appel *et al.* 2001) along the axis of the fibril on the outside of the fibril and would interact favourably with water molecules through hydrogen-bonding. This covalent cross-linking by the formaldehyde would prevent adjacent trimers from dissociating from each other in the fibril and thus inhibit the conversion of fibrils back into 14–28 PrP oligomers within the PL bilayer. This would prevent the 10- to > 100-fold increase in infectivity observed by Gabizon *et al.* (1987, 1988) on dispersion of rods into liposomes.

Formaldehyde treatment appears to increase the IP consistently across four log-dilutions (Fig. 1). At first glance, this observation appears difficult to reconcile with the data of Silveira *et al.* (2005) which show that the IP is similar to both the 14–28 PrP oligomers and the larger fibrils, only increasing for particles smaller than 5 PrP molecules (Table 1). Thus, on the basis of the data of Silveira *et al.* (2005), the IP would be expected to be unaffected by any treatment which altered the relative contributions from 14 to 28 PrP oligomers and the larger aggregates. However, the obvious difference between the aggregates in the study of Silveira *et al.* (2005) and those of Brown *et al.* (2000) presented in Fig. 1 is that in the former the aggregates are held together by noncovalent protein/protein interactions (as shown for the fibrils in Govaerts *et al.* 2004) while in the latter, the aggregates are covalently cross-linked by formaldehyde. Thus, it could be argued that the increase in IP observed with formaldehyde fixation is simply because of the time required for those covalent cross-links to be broken allowing release of the infectious 14–28 PrP oligomers and their integration into the host cell lipid bilayer membranes. For the rods, this dispersion is reversible (Gabizon *et al.* 1988). The time for this process would be constant and independent of dose, thus explaining the constant difference in IP for formaldehyde-treated and untreated brain (Fig. 1). The increase in IP with decreasing dose is modelled by Kulkarni *et al.* (2003).

Computer simulation of effect of formaldehyde on the dose–response

Formaldehyde not only shifts the ID_{50} by the order of three-logs, but also broadens the dose–response (Fig. 1). Thus, in the untreated brain homogenate, the proportion of hamsters infected falls off in just in a single log-dilution. In contrast, for formaldehyde-treated brain homogenate, the proportion of hamsters infected falls off over at least four-logs. The objective of the computer simulation is to test the theory that formaldehyde reduces the infectivity by cross-linking highly infectious particles (fraction 12) into larger aggregates or fibrils of lower-specific infectivity (fraction 21). According to Silveira *et al.* (2005), the specific infectivity of the large PrP fibrils (fraction 21) is ~70-fold lower than that of the 14–28 PrP oligomers (fraction 12). Mathematically, the risk from a given dose, N, of each particle (i.e. 14 – 28 PrP oligomers on one hand or large fibrils on the other hand) is given by:

$$p = 1 - (1 - r)^N \qquad (1)$$

where r is the probability of infection from a single such particle. For the purpose of the computer simulation, it is assumed that the untreated material contains both highly infectious 14–28 PrP oligomers (fraction 12) with a probability, r, of initiating infection of 0·1, together with larger aggregates or fibrils (fraction 21) which are 100-fold less infectious ($r = 0{\cdot}001$). This reflects the 70-fold reduction observed by Silveira *et al.* (2005), and also the 10

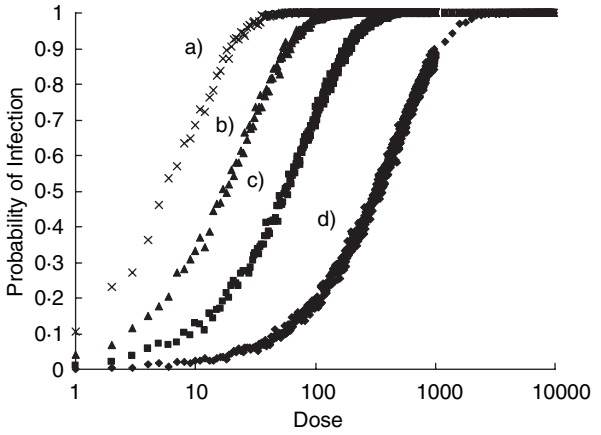

Figure 2 Computer simulation of dose–response from challenge of mixed doses of varying proportions: (a) 98% $r = 0{\cdot}1$, 2% $r = 0{\cdot}001$; (b) 34% $r = 0{\cdot}1$, 66% $r = 0{\cdot}001$; (c) 10% $r = 0{\cdot}1$. 90% $r = 0{\cdot}001$; (d) 1% $r = 0{\cdot}1$, 99% $r = 0{\cdot}001$, where r is the probability of infection from a single unit as described by eqn 1.

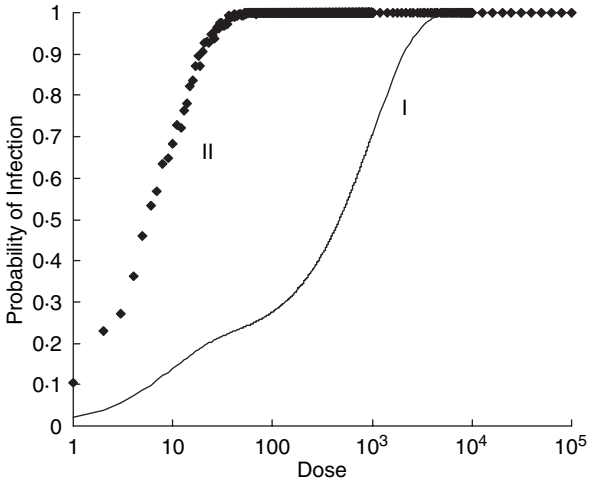

Figure 3 Between-host variation. (I) Two component negative exponential dose–response curve (eqn 2) with $f_1 = 0{\cdot}2$, $f_2 = 0{\cdot}8$, $r_1 = 0{\cdot}1$ and $r_2 = 0{\cdot}001$, representing two host subpopulations with differing susceptibilities. (II) For comparison simulation of mixed dose comprising 98% highly infectious particles ($r = 0{\cdot}1$) and 2% less infectious particles ($r = 0{\cdot}001$).

to > 100-fold increase observed by Gabizon *et al.* (1988) on dispersing rods into liposomes.

The approach for the simulation is to model the shapes of the dose–response curve with differing proportions of the highly infectious 14–28 PrP oligomer particles ($r = 0{\cdot}1$) and the less infectious large fibrils ($r = 0{\cdot}001$). The effect of formaldehyde is modelled by increasing the proportion of less infectious aggregates relative to the highly infectious particles. The simulation programme was written in the C programming language and was based on that developed previously (Gale 2006a) to model the number of *Salmonella* cells in a given dose initiating infection. The difference here is that each dose is comprised of particles with two different probabilities of initiating infection. For a given dose, the simulation was repeated in 1000 hosts, and the proportion of hosts infected plotted against dose (Fig. 2). For each host (for the given dose), the composition in terms of the two particle types was drawn by using the random number generator. This was repeated 1000 times for each dose. Thus for line C in Fig. 2, a dose of 1 particle had a 10% chance of being the highly infectious particle and a 90% chance of being the less infectious particle. So for 1000 hosts, 100 hosts on average would receive the more infectious particle, and 900 hosts the less infectious particle. For higher doses, e.g. 100 particles, on average, a dose would comprise 10 of the more infectious particles, and 90 of the less infectious. It is apparent from the simulation in Fig. 2 that decreasing the proportion of highly infectious particles from 98% to 1% simply shifts the ID_{50} and does not appear to alter the slope of the curve. It is concluded that the change in the shape of the dose–response curve with formaldehyde-fixation (Fig. 1) is not simply because of aggregating highly infectious particles into aggregates of low infectivity.

Shape of dose–response for formaldehyde-fixed brain homogenate reflects 'between hamster' variation

An alternative explanation which better approximates the observed broadening of the dose–response is that there is heterogeneity between hamsters in their susceptibility to formaldehyde-treated brain homogenate. This is shown in Fig. 3 using a two component negative exponential dose–response model (eqn 2) reflecting the existence of two different hamster subpopulations.

$$p = f_1\left(1 - e^{-r_1 N}\right) + f_2\left(1 - e^{-r_2 N}\right) \qquad (2)$$

For the purpose of demonstration, it is assumed that one subpopulation accounting for 20% ($f_1 = 0{\cdot}2$) of the total hamsters is highly susceptible to infection by formaldehyde-fixed brain ($r_1 = 0{\cdot}1$), while the second subpopulation, which accounts for 80% ($f_2 = 0{\cdot}8$) of the hamsters is more resistant ($r_2 = 0{\cdot}001$). This dose–response curve (line I in Fig. 3) resembles the shape of the dose–response for the formaldehyde-fixed brain (Fig. 1) in being broadened around the ID_{50}. In contrast, the dose–response curve simulated for a mixed challenge dose comprising 98% highly infectious particles ($r = 0{\cdot}1$) and 2% less infectious particles ($r = 0{\cdot}001$) is very steep (line II in Fig. 3) resembling more that for the untreated brain homogenate. A possible explanation for the existence of two hamster subpopulations which differ in their susceptibility to formaldehyde-fixed brain is the presence (or

deficiency) of an enzyme which cleaves formaldehyde cross-links, for example. In effect, therefore, some hamsters are better able to reverse the cross-linking effect of formaldehyde, and are therefore more susceptible.

This explanation based on two hamster subpopulations is analogous to avermectin toxicity in CF-1 mice (Lankas *et al.* 1997). Avermectin is an insecticide and subject to toxicity testing (JMPR 1997). A subpopulation of CF-1 mice is unusual in its extreme sensitivity to the avermectins, with neurotoxicity occurring at very low doses (Lankas *et al.* 1997). The difference between subpopulations of CF-1 mice in avermectin sensitivity is due to P-glycoprotein, which is a membrane transport protein that pumps toxic molecules out and contributes to the effectiveness of both the intestinal and the blood–brain barriers. Lankas *et al.* (1997) reported that the sensitive population of CF-1 mice are deficient in P-glycoprotein in both the intestine and brain capillary endothelium. In contrast, avermectin-insensitive CF-1 mice showed abundant levels of P-glycoprotein in these tissues, and tolerated doses at least 50-fold higher than the minimum toxic dose in the sensitive subgroup. Indeed, radiolabelled avermectin levels were much higher in the brains of the P-glycoprotein-deficient mice than the insensitive mice, thus accounting for neurotoxicity at low doses. About 17% of CF-1 mice are highly sensitive to avermectin (JMPR 1997). The existence of two subpopulations of CF-1 mice which differ by 50- to 100-fold in sensitivity to avermectin explains the heterogeneity in the dose–response, giving a two component dose–response model (similar to line I in Fig. 3). On this basis, the JMPR (1997) concluded that CF-1 mice are an inappropriate model for studying avermectin toxicity. The same conclusion could be made for titrating scrapie infectivity in formaldehyde-treated brain using hamster bioassay.

It is proposed here that although formaldehyde treatment shifts the ID_{50} to higher doses (Fig. 1), suggesting inactivation, there is in fact no inactivation at all. Formaldehyde does indeed convert highly infectious particles ($r = 0{\cdot}1$ in eqn 1) into larger, less infectious aggregates ($r = 0{\cdot}001$ in eqn 1). However, this process is reversible, and the infectivity is preserved, as demonstrated by those hamsters better able at breaking the cross-links (so releasing highly infectious 14–28 PrP oligomers from the larger aggregates).

The effect of formaldehyde on IP (Fig. 1) is more difficult to explain. The IP is similar for both highly infectious 14–28 PrP oligomers and for larger fibrils (Table 1). Although this is consistent with the IP changing in harmony with dose for both untreated and formaldehyde-treated brain (Fig. 1), it might be expected that hamsters more efficient at releasing the 14–28 PrP oligomers from the cross-linked aggregates might show shorter IPs, than the more resistant hamsters. This is not the case as shown in Fig. 1. It is perhaps not surprising that formaldehyde affects the IP because formaldehyde will react with the oligosaccharide and it is known that glycosylation of the host PrP^C can influence IP and strain determination (Manson *et al.* 2006) and also the amount of PrP^C bound to PrP^{Sc} (Priola and Lawson 2001). Information is needed on the role of the *N*-linked oligosaccharide in the highly infectious 14–28 PrP oligomers which have only recently been identified (Silveira *et al.* 2005). TSE infection is a two stage process and the IP is the sum of the lag phase and the exponential phase (Kulkarni *et al.* 2003). According to the model of Kulkarni *et al.* (2003), the lag phase is controlled by a number of parameters, including co-ordination state of the PrP molecules in the aggregates. Undoubtedly, this would be affected by formaldehyde, as perhaps would the clearance ratio, and the rate of growth of the seed. It is recommended that the model of Kulkarni *et al.* (2003) is used to model the effect of formaldehyde on IP.

Evidence for the involvement of lipid in the nucleation seed

Protein/protein interactions as an alternative for the 'second component'

The experimental data of Taylor *et al.* (2002) and Somerville *et al.* (2002) do not necessarily support the existence of a second component. Indeed, the concept of a nucleation seed held together entirely be protein/protein interactions could equally well explain the inactivation properties observed by Taylor *et al.* (2002) and Somerville *et al.* (2002). Thus heat, SDS and NaOH would be effective in breaking down the noncovalent protein/protein interactions which exist between PrP molecules and which hold the nucleation seed together. The strength of those protein/protein interactions would reflect the 3D structure of the PrP molecule, and not its primary amino acid sequence (i.e. PrP genotype). Thus, thermostability would be independent of PrP genotype as observed by Taylor *et al.* (2002). Similarly proteinase K resistance could map to a different part of the molecule other than those parts involved in PrP/PrP interactions and controlling thermostability; thus explaining the observations of Somerville *et al.* (2002). Indeed, in the 2D array structure proposed in Fig. 3d of Govaerts *et al.* (2004), there is a scope for protein/protein interactions between the α-helices of adjacent trimers within the plane. Evidence in support of protein/lipid interactions is now reviewed.

Molecular dimensions from biophysical studies

One line of evidence in support of the prion/lipid hypothesis is that dispersing prion rods into PL bilayer

liposomes increases the infectivity by 10- to > 100-fold (Gabizon *et al.* 1987, 1988). This is similar to the difference in specific infectivity between large fibrils and the 14–28 PrP oligomers (fraction 12) reported by Silveira *et al.* (2005). It is tempting to speculate that the 14–28 PrP oligomer particles comprising fraction 12 are actually PrP/PL or SL bilayer complexes with hexagonal 2D structure. The biochemical composition of the 14–28 PrP oligomer particles in fraction 12 was not established by Silveira *et al.* (2005). It would be interesting to test fraction 12 for the presence of amphipathic lipid to confirm or disprove the prion/lipid hypothesis. The particles comprising fraction 12 are 17–27-nm diameter (Silveira *et al.* 2005). At the molecular level, the PrP trimer in 2D crystals (Govaerts *et al.* 2004) is about 6–7-nm diameter. Thus, a 21 × 21 nm 2D fragment would contain about nine trimers, i.e. 27 PrP molecules, which is consistent with the 14–28 PrP molecules estimated by Silveira *et al.* (2005). The large 2D hexagonal arrays (Wille *et al.* 2002) are in the order of 200 nm, but those arrays contain obvious 'gaps' giving the impression of 'compact' units in the order of 20-nm diameter which could break away intact from the main 2D crystal aggregate.

Evidence from inactivation studies supporting the structural contribution of lipid to the infectious unit

Inactivation studies yield a wealth of information on the molecular nature of the TSE infectious unit. Here, a further survey of the literature has given more information supporting the importance of lipid in the infectious unit. Firstly, Bauman *et al.* (2006) reported that the presence of the detergent sarkosyl during a 60-min incubation with NaOH further enhanced PrP^{RES} reduction, completely eliminating the PrP^{RES} signal. Those authors speculated that detergent may liberate lipid membrane-protected PrP^{Sc} to improve access to NaOH, which can then inactivate PrP^{Sc} by altering its structure. In effect, the sarkosyl would disrupt the protein/lipid interactions releasing PrP molecules into micelles, which are then more susceptible to attack by alkali. Secondly, Appel *et al.* (2001) demonstrated that the presence of lipids increased the heat stability of prion rods, especially at lower temperatures. This supports the prion/lipid hypothesis. Prion rods have very little lipid (as discussed above) and lower thermostability than in the presence of lipid. It is not clear exactly what is the lipid composition of the bovine bone fat used by Appel *et al.* (2001) to stabilize the rods, but presumably it includes both PL and SL in addition to triacylglycerols. Thirdly, Taylor *et al.* (1998) demonstrated that organic solvents (hexane, heptane, perchloroethylene and petroleum ether) had no effect on enhancing the thermal inactivation of 22A scrapie agent or 301 V strain of BSE. Those organic solvents are nonpolar, and although appropriate for solubilizing the neutral fats (Hamilton *et al.* 1992) including triacylglycerols (Lehninger 1975) would not solubilize the amphipathic lipids, which have charged polar headgroups (in addition to hydrophobic fatty acyl chains). Thus, all PLs contain a negatively charged phosphate group, and phosphatidylcholine, for example, has a positively charged trimethylammonium group (Lehninger 1975). Similarly, the most abundant SL in the tissues of higher animals is the sphingomyelins, which contain charged phosphorylethanolamine or phosphorylcholine as their polar headgroups (Lehninger 1975). Such charged groups have strongly-bound water molecules, the entropy of which would increase in a solvent such as hexane. Thus, more polar solvents, such as chloroform/methanol/water, are typically used for solubilizing polar PLs (Hamilton *et al.* 1992). The solubility of polar lipids is low in hydrocarbon solvents such as hexane, and petroleum ether alone while recovering all triacylglyceride, only recovered a very small proportion of polar lipids from ground beef (Tanamati *et al.* 2005). In conclusion, the failure of organic solvent to enhance thermal inactivation is not inconsistent with amphipathic protein/lipid interactions playing a role in stabilizing the nucleation seeds. An experiment along the lines of Taylor *et al.* (1998) in which chloroform/methanol/water enhanced thermal inactivation would thus lend support to the importance of amphipathic lipid.

Thermal changes observed in protein structure by FT-IR spectroscopy occur at much lower temperatures than for inactivation of infectivity as determined by bioassay

According to the prion/lipid hypothesis, thermostability is controlled by the strength of lipid/protein interactions (Gale 2006a). Evidence in favour of protein-only contacts controlling thermostability comes from recent Fourier-transform infra red (FT-IR) spectroscopy studies by Spassov *et al.* (2006). This, however, may reflect the fibrils and not the highly infectious 14–28 PrP oligomers. FT-IR studies have demonstrated that the secondary structure of the PrP molecule differs characteristically for different TSE strains for various TSE agents (Spassov *et al.* 2006), and that strain differences were reflected by variations in β-sheet and other amide I components. (The amide I mode originates from the carbonyl stretching frequency of the peptide bonds in the polypeptide backbone). Spassov *et al.* (2006) have used FT-IR to investigate the thermostability of different TSE strains, and showed that a strain-specific response to heat treatment is associated with strain specific thermostability of distinct secondary structure elements. It is unclear, however, as to which PrP aggregates (see Table 1) Spassov *et al.* (2006)

conducted their experiments on. Ideally, to match FT-IR secondary structure data with temperature inactivation data for infectivity from bioassay, Spassov *et al.* (2006) should be studying the most infectious PrP particles (i.e. the 14–28 PrP oligomers identified by Silveira *et al.* (2005)). In all likelihood, however, the PrP^{Sc} purification method used by Spassov *et al.* (2006) isolated PrP fibrils, which have very little lipid associated with them as discussed above. In conclusion, therefore, while temperature-dependent structural changes may be detected in the PrP secondary structure by FT-IR, these may reflect the less infectious rods and not the relevant, highly infectious 14–28 PrP oligomers. Indeed if the 14–28 PrP oligomers are PrP/PL complexes, then they may have completely different thermostabilities because of protein/lipid interactions in 2D hexagonal arrays, compared with fibrils, where protein/protein contacts predominate. Thus, the changes in secondary structure determined by FT-IR (Spassov *et al.* 2006) exhibited greatest sensitivity to temperature at much lower temperatures than reported for loss of infectivity as determined by bioassay. For example, Somerville *et al.* (2002) reported that substantial inactivation of infectivity (measured by intracerebral bioassay) first occurred (inflection points) at temperatures of 82 and 97°C for ME7 and 22A scrapie strains, respectively. In contrast, Spassov *et al.* (2006) reported greatest sensitivity to changes in secondary structure at 58 and 65°C for ME7 and 22A scrapie strain, respectively. It should be noted that the inflection point reported by Somerville *et al.* (2002) represents the temperature at which infectivity begins to be inactivated, while the temperatures of Spassov *et al.* (2006) are midpoints, and the 'inflection points' would be lower still.

Using molecular evidence to support risk assessment assumptions

Survival of 263 K strain of scrapie at 600°C

Brown *et al.* (2000) demonstrated that a very small proportion ($\sim 10^{-9}$) of 263 K strain of scrapie infectivity survived for up to 15 min at 600°C (ashing and dry heat). Thus, although such treatments give 9-log reductions, it is apparent that minute fractions do survive in the glowing ash. As the 14–28 PrP oligomer is the most infectious particle (Silveira *et al.* 2005), survival of just one of these particles may be sufficient to initiate infection with high probability through intracerebral challenge of the ash. Indeed, the work of Silveira *et al.* (2005) demonstrates that survival of large aggregates and fibrils would not be required. Furthermore, at pointed out by Silveira *et al.* (2005), treatments which disaggregate amyloid deposits may do more harm than good through the production of small but highly infectious 14–28 PrP oligomers. It is possible that the ashing experiments of Brown *et al.* (2000) actually produced some of these small aggregates through incomplete combustion of larger aggregates. Moreover, the 2D hexagonal structure would undoubtedly add some protection to the PrP^{Sc} against heat and carbon has been reported to partially protect TSE infectivity at autoclave temperatures (Taylor 1991). As the unheated hamster brain homogenate contained $10^{9{\cdot}9}$ ID_{50} g^{-1} (Brown *et al.* 2000), the combustion process would need to be 100% efficient to eliminate all the infectivity. For the purpose of environmental risk assessment, the important point is that ~9-logs of infectivity were destroyed by the ashing process. The results of Brown *et al.* (2000) demonstrate that for risk assessment purposes, the main factor to consider in burning or incineration of TSE-infected carcasses is the proportion that remains unburnt at the operational efficiency level. This in effect represents a by-pass and is easily accommodated in risk assessments based on an arithmetic mean inactivation (Gale 2004).

More data supporting the assumptions regarding environmental behaviour of TSE agent in the aquatic environment

Environmental transmission of TSEs

Sheep scrapie and cervid CWD (Williams and Young 1992) are unique among TSEs because epizootics can be sustained by horizontal transmission (see Johnson *et al.* 2006). Both infected animals and environments apparently contaminated with the causative agent contribute to scrapie epidemics (Miller *et al.* 2004). Indeed, Miller *et al.* (2004) demonstrated that under experimental conditions, mule deer became infected in two of three paddocks containing naturally infected deer, in two of three paddocks where infected deer carcasses had decomposed *in situ* ~1·8 years earlier, and in one of three paddocks where infected deer had last resided 2·2 years earlier. Miller *et al.* (2004) concluded that indirect transmission and environmental persistence of infectious prions will complicate efforts to control CWD and perhaps other animal prion diseases. Miller *et al.* (2004) note that in contrast to CWD and scrapie, BSE does not appear to be contagious in cattle, with the epidemic being sustained artificially through exposure to feed contaminated with infected bovine tissues. There is, however, no evidence that cattle could not be infected with BSE through environmental routes if remains or residues of bovine brain or spinal cord, for example, were introduced to agricultural land. Indeed, transmission of BSE through application of composted catering waste (Gale 2004) and sewage sludge (Gale and Stanfield 2001) is theoretical, albeit with negligible predicted risks. In this respect, it remains appropriate

to review all new data (both epidemiological and molecular biophysical) which affect the assumptions made in those BSE risk assessments.

TSE infectivity binds to soil minerals

Johnson *et al.* (2006) concluded that PrP^{Sc} released into soil environments may be preserved in a bioavailable form, perpetuating prion disease epizootics and exposing other species to the infectious agents. They examined the potential for soil to serve as a TSE reservoir by studying the interaction of PrP^{Sc} with common soil minerals. They demonstrated substantial PrP^{Sc} adsorption to clay minerals, and soil samples. The interaction between PrP^{Sc} and montmorillonite clay was strong, making desorption of the protein difficult. Despite cleavage and avid binding, PrP^{Sc} bound to montmorillonite clay remained infectious. On this basis, they postulated that an environmental reservoir of TSE infectivity contributes to the natural transmission of TSEs in sheep, deer and elk. Reassuringly, the results of Johnson *et al.* (2006) support the assumptions used previously in environmental risk assessments for BSE in drinking water (Gale *et al.* 1998), sewage sludge (Gale and Stanfield 2001) and composted catering waste containing meat (Gale 2004). Those assumptions were that:

- TSE infectivity binds to particulate matter, and will therefore partition with the particulate matter in treatment processes such as drinking water treatment; and
- TSE infectivity does not decay in the aquatic environment.

They were made on the basis of the amphipathic properties of PrP, and its resistance.

The main concern, however, with the risk assessment for cattle grazing on land treated with sewage sludge (Gale and Stanfield 2001) or composted catering waste (Gale 2004) regards the use of a dose–response model (eqn 1) for bovines based on a bovine oral ID_{50} of 0·1 g of BSE-infected bovine brain. It is now well documented (Lasmézas *et al.* 2005) that a proportion of cattle, at least, are very susceptible with an oral $ID_{50} < 0{\cdot}001$ g of brain (Gale 2006a). It would have been more appropriate to use a bovine oral ID_{50} of 0·001 g in those risk assessments, as was calculated back in 1997 from consideration of the known intracerebral infectivity in mice and the cow-to-mouse species barrier (Gale 2006b).

Molecular considerations confirm that the data of Brown and Gajdusek (1991) do not necessarily reflect decay in the soil

The 2D hexagonal crystalline arrays in Fig. 1a of Wille *et al.* (2002) are in the order of 200–300 nm and would therefore pass through the 450 nm (0·45 μm) pores in the filters used by Brown and Gajdusek (1991). The 14–28 PrP oligomers which are most infectious with respect to PrP content are even smaller in the region of 20 nm (Silveira *et al.* 2005). As argued previously (Gale and Stanfield 2001; Gale 2006b), the loss of 98·3–99·7% of scrapie infectivity after 3-year burial in soil observed by Brown and Gajdusek (1991) could be either due to decay or to surviving PrP^{Sc} sticking to soil particle and not being assayed. Indeed, the PrP^{Sc} aggregation state may be different in the soil after 3 years compared with the positive control. This is because any lipids in the 14-28 PrP oligomers would be preserved in the positive control maintained at −70°C for the 3 years. In contrast, degradation of those PLs in the soil environment over the 3-year period could expose amphipathic regions on the PrP^{Sc} enabling it to bind to soil particles with great affinity. Any PrP^{Sc} attached to soil particles would not be able to pass through the 0·45-μm filter. Therefore, the failure to recover all the infectivity after 3 years could simply be due to its binding to the soil as observed by Johnson *et al.* (2006).

Acknowledgements

I thank Professor Tony Watts at the Biochemistry Department, University of Oxford for inspiration, support and encouragement while supervising my D. Phil. on bacteriorhodopsin/phospholipid interactions during the late 1980s.

References

Anderson, R.M., Donnelly, C.A., Ferguson, N.M., Woolhouse, M.E.J., Watt, C.J., Udy, H.J., MaWhinney, S., Dunstan, S.P. *et al.* (1996) Transmission dynamics and epidemiology of BSE in British cattle. *Nature* **382**, 779–788.

Appel, T.R., Wolff, M., von Rheinbaben, F., Heinzel, M. and Riesner, D. (2001) Heat stability of prion rods and recombinant prion protein in water, lipid and lipid-water mixtures. *J Gen Virol* **82**, 465–473.

Bauman, P.A., Lawrence, L.A., Biesert, L., Dichtelműller, X., Fabbrizzi, F., Gajardo, R., Grőner, A., Jorquera, J.I. *et al.* (2006) Critical factors influencing prion inactivation by sodium hydroxide. *Vox Sang* **91**, 34–40.

Blaurock, A.E. and Stoeckenius, W. (1971) Structure of the purple membrane. *Nature* **233**, 152–155.

Brown, P. and Gajdusek, D. C. (1991) Survival of scrapie virus after 3 years' internment. *Lancet* **337**, 269–270.

Brown, P., Liberski, P.P., Wolff, A. and Gajdusek, D.C. (1990) Resistance of scrapie infectivity to steam autoclaving after formaldehyde fixation and limited survival after ashing at 360°C: practical and theoretical implications. *J Infect Dis* **161**, 467–472.

Brown, P., Rau, E.H., Johnsom, B.K., Bacote, A.E., Gibbs, C.J. and Gajdusek, D.C. (2000) New studies on the heat resistance of hamster-adapted scrapie agent: threshold survival after ashing at 600°C suggest an inorganic template of replication. *Proc Natl Acad Sci USA* **97**, 3418–3421.

Caughey, B. and Lansbury, P.T. (2003) Protofibrils, pores, fibrils, and neurodegeneration: separating the responsible protein aggregates from the innocent bystanders. *Ann Rev Neurosci* **26**, 267–298.

Comer, P.J. and Huntly, P.J. (2004) Exposure of the human population to BSE infectivity over the course of the BSE epidemic in Great Britain and the impact of changes to the Over Thirty Month Rule. *J Risk Res* **7**, 523–543.

Dietz, K., Raddatz, G., Wallis, J., Műller, N., Zerr, I., Duerr, H.-P., Lefèvre, H., Seifried, E. *et al.* (2007) Blood transfusion and spread of variant Creutzfeldt–Jakob disease. *Emerg Infect Dis* **13**, 89–96.

Gabizon, R., McKinley, M.P. and Prusiner, S.B. (1987) Purified prion proteins and scrapie infectivity copartition into liposomes. *PNAS USA* **84**, 4017–4021.

Gabizon, R., McKinley, M.P., Groth, D.F., Kenaga, L. and Prusiner, S.B. (1988) Properties of scrapie prion protein liposomes. *J Mol Chem* **263**, 4950–4955.

Gale, P. (1993) Comparison of bacteriorhodopsin/phospholipid interactions in DMPC and DMPG bilayers: an electron spin resonance spectroscopy and freeze-fracture electron microscopy study. *Biochem Biophys Res Commun* **196**, 879–884.

Gale, P. (2004) Risks to farm animals from pathogens in composted catering waste containing meat. *Vet Rec* **155**, 77–82.

Gale, P. (2006a) The infectivity of transmissible spongiform encephalopathy agent at low dose: the importance of phospholipid. *J Appl Microbiol* **101**, 261–274.

Gale, P. (2006b) BSE risk assessments in the UK: a risk tradeoff? *J Appl Microbiol* **100**, 417–427.

Gale, P. and Stanfield, G. (2001) Towards a quantitative risk assessment for BSE in sewage sludge. *J Appl Microbiol* **91**, 563–569.

Gale, P., Young, C., Stanfield, G. and Oakes, D. (1998) Development of a risk assessment for BSE in the aquatic environment. *J Appl Microbiol* **84**, 467–477.

Govaerts, C., Wille, H., Prusiner, S.B. and Cohen, F.E. (2004) Evidence for assembly of prions with left-handed β-helices into trimers. *PNAS USA* **101**, 8342–8347.

Grigorieff, N., Beckmann, E. and Zemlin, F. (1995) Lipid location in deoxycholate-treated purple membrane at 2.6 Å. *J Mol Biol* **254**, 404–415.

Hamilton, S., Hamilton, R.J. and Sewell, P.A. (1992) Extraction of lipids and derivative formation. In *Lipid Analysis – A Practical Approach* ed. Hamilton, R.J. and Hamilton, S. pp. 13–64. Oxford: IRL Press.

Henderson, R. and Unwin, P.N. (1975) Three-dimensional model of purple membrane obtained by electron microscopy. *Nature* **257**, 28–32.

Henderson, R., Baldwin, J.M., Ceska, T.A., Zemlin, F., Beckmann, E. and Downing, K.H. (1990) Model for the structure of bacteriorhodopsin based on high-resolution electron cryo-microscopy. *J Mol Biol* **213**, 899–929.

Hornemann, S., Schorn, C. and Wűthrich, K. (2004) NMR structure of the bovine prion protein isolated from healthy calf brains. *EMBO Rep* **5**, 1159–1164.

Ironside, J.W., Bishop, M.T., Connolly, K., Hegazy, D., Lowrie, S., Le Grice, M., Ritchie, D.L., McCardle, L.M. *et al.* (2006) Variant Creutzfeldt–Jakob disease: prion protein genotype analysis of positive appendix tissue samples from a retrospective prevalence study. *Br Med J* **332**, 1886–1188.

JMPR (1997) Joint Meeting on Pesticide Residues. Monographs of Toxicological Evaluation, No. 925. Abamectin (Pesticide residues in food: 1997 evaluations Part II Toxicological & Environmental). Available at http://www.inchem.org/documents/jmpr/jmpmono/v097pr02.htm.

Johnson, C.J., Phillips, K.E., Schramm, P.T., McKensie, D., Aiken, J.D. and Pederon, J.A. (2006) Prions adhere to soil minerals and remain infectious. *PloS Pathog* **2**, 296–302.

Kates, M., Kushwaha, S.C. and Sprott, G.D. (1982) Lipids of purple membrane from extreme. halophiles and of methanogenic bacteria. *Methods Enzymol* **88**, 98–111.

Kazlauskaite, J. and Pinheiro, T.J.T. (2005) Aggregation and fibrillization of prions in lipid membranes. *Biochem Soc Symp* **72**, 211–222.

Kimberlin, R.H. (1996) Bovine spongiform encephalopathy and public health: some problems and solutions in assessing risks. In *Transmissible Subacute Spongiform Encephalopathies: Prion Diseases* ed. Court, L. and Dodet, B. pp. 487–503. Paris: Elsevier.

Kimberlin, R.H. and Wilesmith, J.W. (1994) Bovine spongiform encephalopathy (BSE): epidemiology, low dose exposure and risk. *Ann N Y Acad Sci* **724**, 210–220.

Kulkarni, R.V., Slepoy, A., Singh, R.R.P., Cox, D.L. and Pázmándi, F. (2003) Theoretical modeling of prion diesase incubation. *Biophys J* **85**, 707–718.

Langedijk, J.P.M., Fuentes, G., Boshuizen, R. and Bonvin, A.M.J.J. (2006) Tw-rung model of a left-handed β-helix for prions explains species barrier and strain variation in transmissible spongiform encephalopathies. *J Mol Biol* **360**, 907–920.

Lankas, G.R., Cartwright, M.E. and Unbenhauer, D. (1997) P-glycoprotein deficiency in a subpopulation of CF-1 mice enahnces avermectin-induced neurotoxicity. *Toxicol Appl Pharmacol* **143**, 357–365.

Lasmézas, C.I., Comoy, E., Hawkins, S., Herzog, C., Mouthon, F., Konold, T., Auvré, F., Correia, E. *et al.* (2005) Risk of oral infection with bovine spongiform encephalopathy agent in primates. *Lancet* **365**, 781–783.

Leffers, K.-W., Schell, J., Jansen, K., Lucassen, R., Kaimann, T., Nagel-Steger, L., Tatzelt, J. and Riesner, D. (2004) The structural transition of the prion protein into its pathogenic conformation is induced by unmasking hydrophobic sties. *J Mol Biol* **344**, 839–853.

Lehninger, A.L. (1975) Lipids, lipoproteins and membranes. In *Biochemistry*, 2nd edn. pp. 279–308. New York: Worth Publishers Inc.

Mahfoud, R., Garmy, N., Maresca, M., Yahi, N., Puigserver, A. and Fantini, J. (2002) Identification of a common sphingolipid-binding domain in Alzheimer, Prion and HIV-1 proteins. *J Biol Chem* **277**, 11292–11296.

Manson, J., Barron, R., Hart, P., Tuzi, N. and Bishop, M. (2006) The role of host PrP in control of incubation time. In *Prions* ed. Kiamoto, T. pp. 109–117. Tokyo: Springer Link.

McDonnell, G. and Burke, P. (2003) The challenge of prion decontamination. *Clin Infect Dis* **36**, 1152–1154.

Miller, M.W., Williams, E.S., Hobbs, N.T. and Wolfe, L.L. (2004) Environmental sources of prion transmission in mule deer. *Emerg Infect Dis* **10**, 1003–1006.

Peden, A.H., Head, M.W., Ritchie, D.L., Bell, J.E. and Ironside, J.W. (2004) Preclinical vCJD after blood transfusion in a PRNP codon 129 heterozygous patient. *Lancet* **364**, 527–529.

Priola, S.A. and Lawson, V.A. (2001) Glycosylation influences cross-species formation of protease-resistant prion protein. *EMBO J* **20**, 6692–6699.

Prusiner, S.B. (2004) An introduction to prion biology and diseases. In *Prion Biology and Diseases*, 2nd edn. ed. Prusiner, S.B. pp. 1–87. New York: Cold Spring Harbor Laboratory Press.

Prusiner, S.B., Williams, E., Laplanche, J.-L. and Shinagawa, M. (2004) Scrapie, chronic wasting disease, and transmissible mink encephalopathy. In *Prion Biology and Diseases*, 2nd edn. ed. Prusiner, S.B. pp. 545–595. New York: Cold Spring Harbor Laboratory Press.

Rudd, P.M., Endo, T., Colominas, C., Groth, D., Wheeler, S.F., Harvey, D.J., Wormald, M.R., Serban, H. *et al.* (1999) Glycosylation differences between the normal and pathogenic prion protein isoforms. *PNAS USA* **96**, 13044–13049.

Sabra, M.C., Uitdenhaag, J.C.M. and Watts, A. (1998) General model for lipid-mediated two-dimensional array formation of membrane proteins: application to bacteriorhodopsin. *Biophys J* **75**, 1180–1188.

Silveira, J.R., Raymond, G.J., Hughson, A.G., Race, R.E., Sim, V.L., Hayes, S.F. and Caughey, B. (2005) The most infectious prion protein particle. *Nature* **437**, 257–261.

Somerville, R.A., Oberthűr, R.G., Havekost, U., MacDonald, F., Taylor, D.M. and Dickinson, A.G. (2002) Characterisation of thermodynamic diversity between transmissible spongiform encephalopathy agent strains and its theoretical implications. *J Biol Chem* **277**, 11084–11089.

Spassov, S., Beekes, M. and Naumann, D. (2006) Structural differences between TSE strains investigated by FT-IR spectroscopy. *Biochim Biophys Acta* **1760**, 1138–1149.

Sternberg, B., Gale, P. and Watts, A. (1989) The effect of temperature and protein content on the dispersive properties of bacteriorhodopsin from *H.* Halobium in reconstituted DMPC complexes free of endogenous purple membrane lipids: a freeze-fracture electron microscopy study. *Biochim Biophys Acta* **980**, 117–126.

Sternberg, B., L'Hostis, C., Whiteway, C.A. and Watts, A. (1992) The essential role of specific *Halobacterium halobium* polar lipids in 2D-array formation of bacteriorhodopsin. *Biochim Biophys Acta* **1108**, 21–30.

Tanamati, A., Oliveira, C.C., Visentainer, J.V., Matsushita, M. and de Souza, N.E. (2005) Comparative study of total lipids in beef using chlorinated solvent and low-toxicity solvent methods. *J Am Oil Chem Soc* **82**, 393–397.

Taylor, D.M. (1991) Impaired thermal inactivation of ME7 scrapie agent in the presence of carbon. *Vet Microbiol* **27**, 403–405.

Taylor, D.M. and Fernie, K. (1996) Exposure to autoclaving or sodium hydroxide extends the dose–response curve of the 263 K strain of scrapie agent in hamsters. *J Gen Virol* **77**, 811–813.

Taylor, D.R. and Hooper, N.M (2006) The prion protein and lipid rafts (review). *Mol Membr Biol* **23**, 89–99.

Taylor, D.M. and McConnell, I. (1988) Autoclaving does not decontaminate formol-fixed scrapie tissues. *Lancet*, **1**, 463–1.

Taylor, D.M., Fernie, K., McConnell, I., Ferguson, C.E. and Steele, P.J. (1998) Solvent extraction as an adjunct to rendering: the effect on BSE and scrapie agent of hot solvents followed by dry heat and steam. *Vet Rec* **143**, 6–9.

Taylor, D.M., Fernie, K., Steele, P.J., McConnell, I. and Somerville, R.A. (2002) Thermostability of mouse-passaged BSE and scrapie is independent of host PrP genotype: implications for the nature of the causal agents. *J Gen Virol* **83**, 3199–3204.

Wells, G.A.H. and Wilesmith, J.W. (2004) Bovine spongiform encephalopathy and related diseases. In *Prion Biology and Diseases*, 2nd edn ed. Prusiner, S.B. pp. 595–628. New York: Cold Spring Harbor Laboratory Press.

Wille, H, Michelitsch, M.D., Guenebaut, V., Supattapone, S., Serban, A., Cohen, F.E., Agard, D.A. and Prusiner, S.B. (2002) Structural studies of the scrapie prions protein by electron crystallography. *Proc Natl Acad Sci USA* **99**, 3563–3568.

Williams, E.S. and Young, S. (1992) Spongiform encephalopathies in Cervidae. *Rev Sci Tech* **11**, 551–567.

Wu, D., Zajonc, D.M., Fujio, M., Sullivan, B.A., Kinjo, Y., Kronenberg, M., Wilson, I.A. and Wong, C-H (2006) Design of natural killer T cell activators: structure and function of a microbial glycosphingolipid bound to mouse CD1d. *PNAS USA* **103**, 3972–3977.

